Studying the roles of RhoA and Anillin in *C. elegans* epidermal morphogenesis.

Nellie Fotopoulos

A Thesis

In

The Department

Of Biology

Presented in the Partial Fulfillment of the Requirements

For the Degree of Maters of Science (Biology) at

Concordia University

Montreal, Quebec, Canada

November 19 2012

CONCORDIA UNIVERSITY
School of Graduate Studies

This is to certify that the thesis prepared

By: Nellie Fotopoulos

Entitled: Studying the roles of RhoA and Anillin in C. elegans epidermal morphogenesis.

and submitted in Partial fulfillment of the requirements of the degree of

Master of Science (Biology)

complies with the regulations of the University and meets the accepted standards with respect to originality and quality.

Signed by the final Examining committee:

Dr. Donal Hickey	Chair
Dr. Christopher Brett	Examiner
Dr. Amy Maddox	Examiner
Dr. Catherin Bachewich	External Examiner
Dr. Alisa Piekny	Supervisor

Approved by _____
Chair of the Department or Graduate Program Director

_____2012

_____
Dean of Faculty

ABSTRACT

Studying the roles of RhoA and Anillin in *C. elegans* epidermal morphogenesis.

Nellie Fotopoulos

During development, epidermal morphogenesis encloses the *C. elegans* embryo in a layer of epidermal cells (by dorsal intercalation and ventral enclosure) and lengthens the embryo into the characteristic worm shape (elongation). These processes occur by a combination of cell shape changes, migration and adhesion. Genes that are involved in these events include Rho GTPases, nucleators of F-actin, nonmuscle myosin regulators and the catenin/cadherin complex that mediates junction formation.

Elongation occurs due to actin-myosin mediated contractions within the lateral epidermal cells. Rho kinase (LET-502), a RhoA effector that activates nonmuscle myosin, and myosin phosphatase (MEL-11), which down regulates myosin activity, are required for elongation. Biochemical analyses performed in other organisms predict that RhoA (RHO-1) functions upstream of Rho kinase (LET-502) and nonmuscle myosin in the elongation pathway, however, due to the lack of *rho-1* alleles, genetic tests had not verified this. We used a zygotic null allele of *rho-1* recently generated by the Knockout Consortium to show that *rho-1* is required for elongation. Crosses between *rho-1* and elongation mutants, including *mlc-4* (nonmuscle myosin regulatory light chain), *let-502* (Rho-kinase) and *mel-11* (myosin phosphatase regulatory subunit), confirmed *rho-1* as an upstream regulator of nonmuscle myosin.

Ventral enclosure is the process where ventral epidermal cells migrate over the ventral surface of the embryo and meet at the midline to adhere with their contralateral neighbours. Some of the genes required for ventral enclosure include actin regulators such as Rac, Arp 2/3 and Wave/Scar (which nucleate the formation of branched F-actin to form lamellipodia) and adhesion components including the cadherin/catenin complex. Other genes contribute to ventral enclosure non-autonomously, such as *vab-1* and *vab-2*, which are expressed in specific subsets of neuroblast cells that function as a substrate for the overlying ventral epidermal cells. It is not fully understood how neuroblasts non-autonomously regulate epidermal cell migration. Here, we show that *C. elegans* anillin (ANI-1), a scaffold protein that binds to F-actin and active myosin, is non-autonomously required for ventral enclosure. In *ani-1* RNAi embryos expressing AJM-1::GFP (a marker for epidermal cell junctions), ventral epidermal cells were mis-aligned and failed to adhere at the ventral surface of the embryo. Furthermore, imunostaining revealed that ANI-1 is primarily expressed in dividing neuroblast cells. These data suggest that neuroblasts may mechanically regulate ventral epidermal cell migration, shedding light on one of the mechanisms by which metazoan tissues may form in vivo.

Acknowledgments

I would first off, and most importantly, thank my supervisor Dr. Alisa Piekny. She was a great professor during my undergraduate studies, so much to the point that I found myself taking any course she was teaching. Alisa took me under her wing for my undergraduate thesis project and allowed me to continue in her lab as a graduate student. The skills that she enabled me to develop included learning how to work in a lab, write scientifically, conduct research and get over my fear of public speaking. The most priceless lesson she has taught me however, was one of resilience. Alisa went through some difficult times during my time in her lab and she never left her students behind or gave up on the research we were doing. Having such a dedicated scientist as a supervisor has led me to believe that we can accomplish anything we set our minds to, and for this, I am forever grateful. This would not be complete if I didn't congratulate you on your best achievement yet, baby Ava.

I want to express my gratitude to my committee members, Dr. Amy Maddox and Dr. Chris Brett for their advice and guidance to complete this project.

In the lab, I was fortunate enough to meet exceptional intellectuals. Thank you Madhav for the advice and encouragement but mostly for sticking funny comics on my bench to make us laugh. Thank you Melina for your wisdom, pep talks and confidence boosts. Thank you Tara for the philosophical debates that are much needed during times of high stress. Thank you Yun, for your professionalism while working together and taking care of all the things we need in the lab. Thank you to Chloe, for always helping out any way you can and for all the microscope trainings. Thank you Denise, for your

efficiency, focus and for being a great travelling buddy during our C.elegans conference in Wisconsin.

Dedications

I dedicate the first half of my thesis to my parents, Maria and Zissis Fotopoulos. You raised, nurtured and loved me, but also taxed yourselves greatly for my intellectual, physical and social development. I appreciate all you have done and hope this achievement makes you proud.

The second half of my thesis is dedicated to my fiancé, Steven. Starting a master's can be as easy as starting any project, but going through with it and completing it is another story. Thank you for your much needed support, comfort and encouragement during the final stages of my degree. I love you.

Contribution of Authors

Figure 6: The RhoA pathway was adapted from the model by Dr. Alisa Piekny, Michael Werner and Michael Glotzer.

Figure 8: The Arp2/3 nucleation of F-actin model was adapted from the model by Susan Abmayr and Grace Pavlath.

Figure 9: The figure of anillin homologues was adapted from the model by Dr. Amy Maddox.

Figure 10: The epithelial junctions model was adapted from the model by Dr. Michel Labouesse.

Figure 12: Yun Chen contributed by acquiring micrographs and made the figure.

Figure 13: Dr. Alisa Piekny contributed by taking photos. I prepared the embryos for filming and made the figure.

Figure 15: Denise Wernike and I worked together to obtain a micrograph of the AJM-1::GFP on *ani-1* RNAi embryo.

Figure 16: Yun Chen stained the embryos and acquired the micrographs. Dr. Alisa Piekny contributed by making the figure.

Figure 18: Yun Chen and I acquired micrographs and made the figure together.

Table 1: Yun Chen worked together in acquiring data from the genetic crosses.

Table 4: Denise Wernike and I counted the phenotypes and made the table.

Table 6: Denise Wernike and I performed the epidermal cell counting of embryos.

Table of Contents

List of Figures

List of Tables

Chapter 1. Introduction

Cell shape change, migration and adhesion are all crucial for the formation and homeostasis of eukaryotic tissues. These processes are regulated in response to a combination of internal, tightly regulated pathways and external cues from the surrounding environment. Many types of cell shape change involve regulation of the actin-myosin cytoskeleton, which generates changes in force and tension to alter the cortex. For example, amoebae extend pseudopodia by flowing cytoplasm into actin-concentrated cones formed at the plasma membrane (Bray et al., 1988). This shape change bestows motility, which allows this single-celled organism to obtain food. As another example, mammalian neurons are born round, but then extend long dendrites and axons to form synapses and a complex neuronal network with other neurons (Ahuja et al., 2007). Migrating cells use a combination of shape changes and extension of actin-rich lamellipodia or filipodia to move over a substrate. This type of movement is particularly important for the formation of tissues during development and wound healing, which allows epithelial cells to close around an open injury (Bement et al., 1993). Unfortunately, cell shape change and migration also drive metastasis; the progression of cancer to a highly malignant state as cancer cells lose their tissue-specific identity and travel to secondary locations in the body (Bompard et al., 2005).

1.1. Morphogenesis in *C. elegans* embryos

Morphogenesis is defined as the generation of a new shape. During development, morphogenesis is crucial for the formation of tissues, and particularly the epithelium. To form a single layer of epithelial cells over the entire surface of the embryo, the actin-

myosin cytoskeleton within each cell is regulated to change shape and/or form extensions and must be coordinated between neighbouring cells. The molecular mechanisms that drive cell shape changes and migration during development are still not fully understood. Since the metastasis of cancer cells also involves morphogenetic-like events (and is often coupled with epithelial-mesenchymal transitions), understanding these molecular pathways may also shed light on metastasis.

C. elegans is an excellent model organism to study genes involved in morphogenesis. *C. elegans* are amenable for genetic experiments due to their short life span, large brood size and ability to self fertilize as hermaphrodites, or be outcrossed to males (Brenner, 1974; The *C. elegans* Sequencing Consortium, 1998). In addition, young adult worms can be fed dsRNA to knock down target genes and their transparent embryos can be imaged for phenotypes during development, since the stages of development typically occur in a highly reproducible manner (Sulston and Horvitz, 1977). The fertilized gamete continuously divides until about the 300-cell stage, then undergoes morphogenesis to enclose the embryo in a layer of epidermal cells that constrict and elongate to change the embryo from an ovoid into the long, thin worm shape. These three events; dorsal intercalation, ventral enclosure and elongation will be described in more detail (see below). However, prior to undergoing these morphogenetic events to form the epithelium, the embryo undergoes gastrulation to internalize cells into the embryo for the formation of internal organs.

1.1.1 Gastrulation

Gastrulation occurs ~100-150 minutes after the first division and internalizes the gut, germline and mesoderm (Figure 1). A ventral cleft is formed as a result of these cellular ingressions and is closed by migrating neuroblasts, ectoderm cells that are neuronal precursors. Therefore, both cell shape changes (for cell ingressions) and cell rearrangements (to close the cleft) are essential for gastrulation to successfully occur (Reviewed by Nance et al., 2005). Asymmetric actin-myosin contractions near the apical surface of the E (endoderm) daughter cells, causes them to adopt a wedge-shape, which permits their ingression (Roh-Johnson et al., 2012). Cells accumulate cortical tension by the contraction of actin-myosin filaments, which is followed by apical constrictions to permit apically constricted cells to move together (Roh-Johnson et al., 2012). Ingressing cells become polarized prior to the asymmetric accumulation of active myosin to the apical cortex, to establish 'inner' vs. 'outer' polarity (Anderson et al., 2008; Harrell and Goldstein, 2010). This polarity is established by PAR-3 and PAR-6, which are restricted to the contact-free surfaces of cells, and becomes the apical surface of the ingressing E cells. PAR-3 and PAR-6 are recruited to the cortex by active CDC-42. The RhoGAP PAC-1 restricts the localization of PAR-3 and PAR-6 to the outer cortex of cells by downregulating CDC-42 at the inner cortex. In *pac-1* mutant embryos, PAR-3 and PAR-6 localize to both the inner and outer cortex of cells, which prevents the asymmetric accumulation of myosin at the apical cortex and causes gastrulation defects (Anderson et al., 2008).

1.1.2 Ventral Cleft Closure

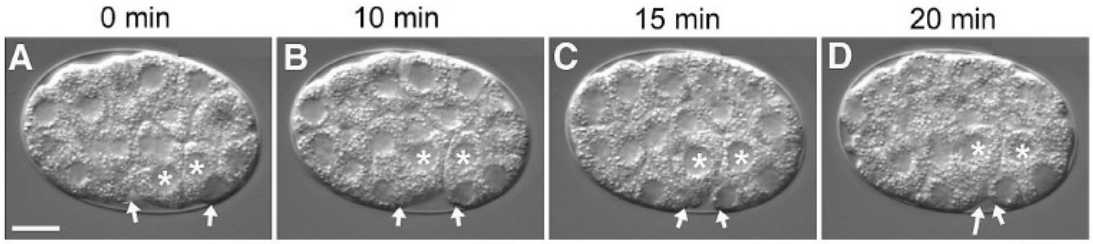

Figure 1. A gastrulating *C. elegans* embryo. Time-lapse, Nomarski images show gastrulation in a wild-type embryo. Time 0 indicates the onset of gastrulation movements (arrowheads). Asterisks mark the endoderm cells to show their movement to a more inward position within the embryo. Figure from Nance et al., (2005).

A ventral cleft remains after gastrulation and its closure occurs approximately 230-290 minutes after the first division. The cleft is closed by migrating neuroblasts from the posterior to anterior end of the embryo (Figure 2; Reviewed by Chisholm and Hardin, 2005). An ephrin-signaling pathway that is transmitted between neighboring cells determines their position (Chin-Sang et al., 1999; Chin-Sang et al., 2000). For example, one subset of cells expresses the VAB-1 tyrosine kinase receptor and the other subset expresses its ligand, VAB-2 (also known as EFN-1; Wang et al., 1999; Chin-Sang et al., 2002). Null *efn-1* mutants take longer for neuroblasts to move towards the cleft, but are able to complete the process and yield no severe phenotypes. Conversely, *vab-1* and *efn-1* double mutants show severe phenotypes and the ventral cleft remains unnaturally large due to the failed migration of neuroblasts (Chin-Sang et al., 2002). Interestingly, mutations in the Wave/Scar complex (regulates branched F-actin filaments; Section 1. 2.2) cause severe defects in the organization of neuroblasts, suggesting that the formation of actin filaments is required for neuroblast cell movements (Withee et al., 2004; Reviewed by Chisholm and Hardin, 2005).

1.1.3 Dorsal Intercalation

Six rows of epidermal cells first appear on the dorsal surface of the embryo around 290 minutes after the first cell division, and the first epidermal morphogenetic event involves intercalation of the dorsal cells to form a single row of cells (Figure 3; Williams-Masson et al., 1998; Chisholm and Hardin, 2005). Dorsal intercalation begins with interdigitation of the two inner rows of epidermal cells on the dorsal surface, which extend from the central axis towards the opposite side of the embryo (Figure 8; Williams-

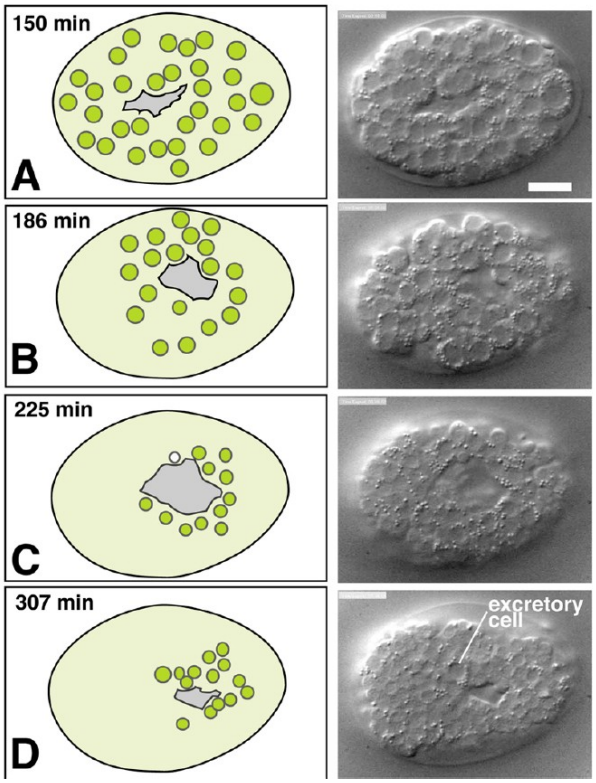

Figure 2. Ventral cleft enclosure in *C. elegans*. Time-lapse, Nomarski images (on right) are shown with cartoon schematics and the time (on left) of ventral cleft closure in a wild-type embryo. Ventral neuroblast cell (green) movements are highlighted. Figure from Chisholm and Hardin, (2005).

Masson et al., 1998; Simske and Hardin, 2001). Dorsal epithelial cells are initially round and become wedge-shaped during interdigitation. After, the cells become rectangular in shape by extending basolateral membrane protrusions composed of actin and microtubules (Williams-Masson et al., 1998). The result is a flat sheet of twenty cells on the back of the embryo where some cells subsequently fuse.

Embryos that fail to complete dorsal intercalation display gut extrusion phenotypes (gut on the exterior, GEX), as the ventral epidermal cells subsequently fail to migrate and enclose the ventral surface of the embryo, leaving the internal contents exposed (Soto et al., 2002). The GEX genes (*gex-2* and *gex-3*) encode components of the Wave/Scar complex, which regulates the formation of short, branched, F-actin filaments for cell migration (Section 1.2.2; Soto et al., 2002). The ability of mutations in these genes to completely block epidermal cell migration emphasizes the importance of F-actin in forming the *C. elegans* epithelium.

1.1.4 Ventral Enclosure

Shortly after dorsal intercalation, ventral enclosure occurs to cover the ventral surface of the embryo in a layer of epidermal cells (Figure 4). The ventral epidermal cells migrate by epiboly over an underlying substrate until they meet at the ventral midline where they adhere with contralateral neighbours (Figure 4; Reviewed by Chisholm and Hardin, 2005). This morphogenetic event can be subdivided into two steps. First, two pairs of anterior leading edge cells migrate towards the ventral midline, where they meet, adhere and subsequently fuse (Figure 4). Lamellipodia/filipodia (actin-rich projections)

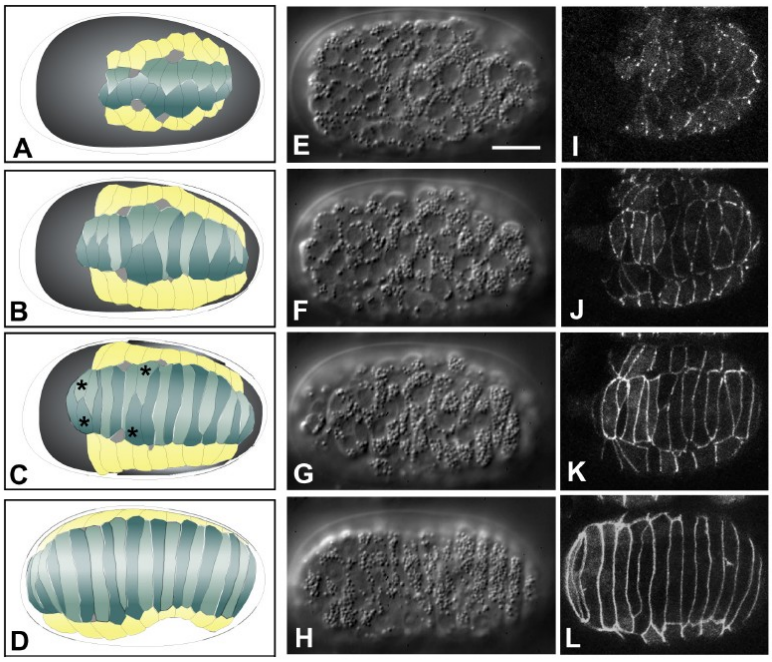

Figure 3. Dorsal intercalation in *C. elegans*. Cartoon schematics (left), Nomarski images (middle) and DLG-1::GFP images (right) show the progression of wild-type embryos undergoing dorsal intercalation. Dorsal cells (green) first form a wedge shape, then interdigitate and extend to cover the dorsal surface in epidermal tissue (alternate cells are shown in dark or light green, and an asterix marks two neighbouring cells that are interdigitating). DLG-1::GFP is a component of adherens junctions that marks epidermal cell boundaries. Figure from Chisholm and Hardin, (2005).

extend from the free-ends of the leading cells to guide their migration towards contralateral neighbouring cells. Not surprisingly, genes required for the migration of ventral epidermal cells and for the formation of these F-actin projections regulate F-actin and include the Rac pathway, Arp2/3, WASp and the Wave/Scar complex (Section 1.2.2; Patel et al., 2008; Quin et al., 2008). The second step involves migration of the posterior ventral pocket cells to close the posterior ventral surface (Figure 4; Chisholm and Hardin, 2005; Zhang et al., 2010). There may be multiple mechanisms for closing the ventral pocket, one of which may involve a contractile-mechanism to draw the pocket cells closed in a purse-string like-manner. Another mechanism requires the formation of a bridge between specific subsets of opposing P cells. The formation of this bridge is dependent on cellular extensions, which are initiated by the VAB-1/Eph receptor-signaling pathway in the underlying neuroblasts (Ikegami et al., 2012).

The ventral epidermal cells must be precisely aligned with their contralateral partners on either side of the ventral midline to form adherens junctions. Genes that regulate cell adhesion include those that encode the cadherin/catenin complex (*hmr-1*, *hmp-1* and *hmp-2;* Section 1.2.5; Costa et al., 1998; Raich et al., 1999). Mutations in these genes prevent the adhesion of ventral epidermal cells, causing rupturing to occur during subsequent steps of embryogenesis. Embryos with more severe adhesion phenotypes rupture immediately, while milder phenotypes include larva that display abnormal body morphologies, such as Hammerhead (Hmr) and Humpback (Hmp) phenotypes (Chisholm and Hardin, 2005).

Ventral epidermal cells also require a substrate for their successful migration to the ventral midline. VAB-1 and VAB-2/EFN-1 are expressed in the underlying

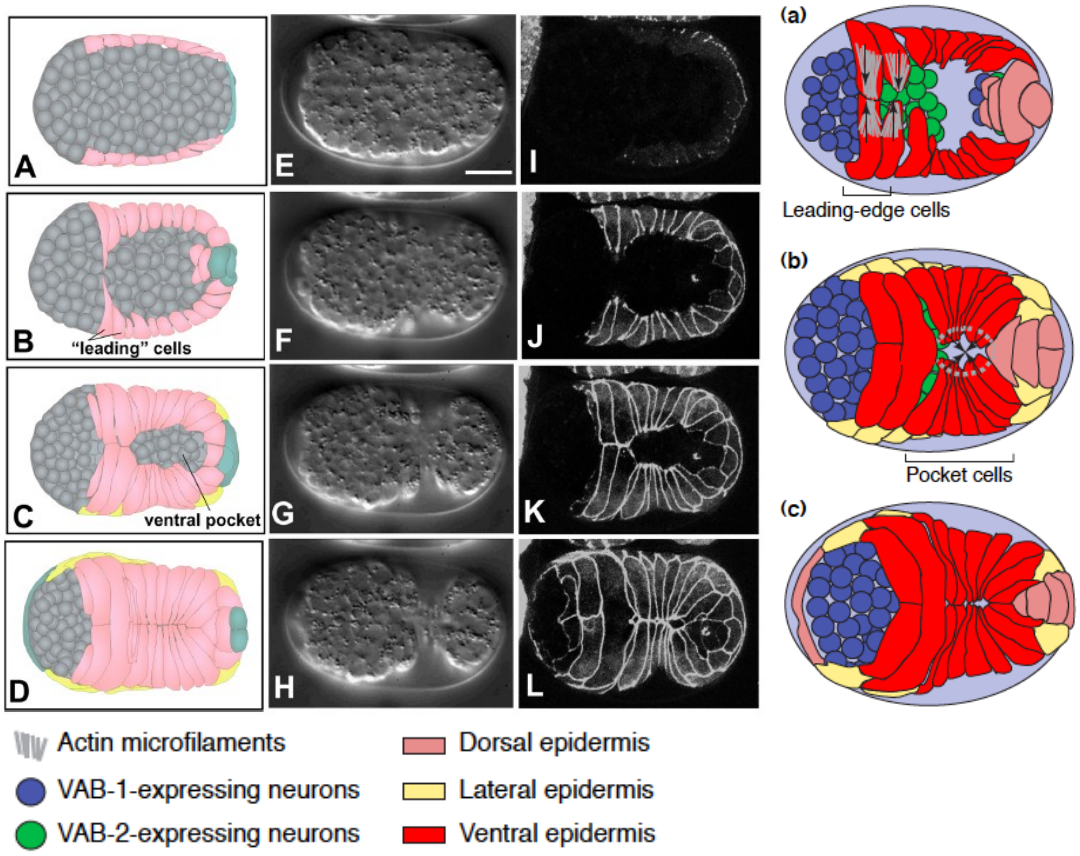

Figure 4. Ventral enclosure in *C. elegans*. The panel on the left shows cartoon schematics (far left), Nomarski images (middle) and DLG-1::GFP images (right) of a wild-type embryo undergoing ventral enclosure. Leading edge cells (pink) migrate first and meet at the ventral midline concomitant with the migration of cells surrounding the posterior ventral pocket. The right panel shows cartoon schematics of an embryo undergoing ventral enclosure, but highlights the underlying neuroblasts that express VAB-1 (purple) or VAB-2 (green), and act as a substrate for migration of the ventral epidermal cells (red). Figure adapted from Chisholm and Hardin, (2005) and Chin-Sang & Chisholm, (2000).

neuroblasts, but not in the epidermal cells (Chin-Sang et al., 1999; Wang et al., 1999; Chin-Sang et al., 2002). Ephrin signaling ensures that VAB-1 and EFN-1 cells sort away from each other, creating an anterior and posterior enrichment of VAB-1-expressing cells and an enrichment of EFN-1-expressing cells in the middle of the embryo (Chin-Sang et al., 1999; Wang et al., 1999; Chin-Sang et al., 2002). Mutations in either *vab-1* or *efn-1* prevent the proper sorting of these cells and cause ventral enclosure phenotypes, supporting the non-autonomous role of neuroblasts in ventral enclosure (Chin-Sang et al., 1999; Wang et al., 1999; Chin-Sang et al., 2002). It is not clear how these cells guide the overlying epidermal cells.

1.1.5 Elongation

One of the last morphogenetic events that occurs during embryogenesis is elongation. During elongation (390-520 minutes after fertilization), the lateral epidermal cells, seam cells, change from a cuboidal to a cylindrical shape and increase the length of the embryo by 4-fold (Figure 5; Priess et al., 1986; Piekny et al., 2003; Chisholm and Hardin, 2005). Elongation primarily occurs by the myosin-mediated contraction of actin filaments within the seam cells, causing them to constrict and extend their shape. The surrounding dorsal and ventral cells remain in a relaxed state (Figure 5; Priess et al., 1986; Wissmann et al., 1997; Piekny et al, 2003). This combination of lateral contractions versus dorsal/ventral relaxations allows the seam cells to lengthen while pulling the surrounding cells with them.

Rho kinase/LET-502 drives contraction likely by phosphorylating MLC-4, the nonmuscle myosin regulatory light chain, to promote the formation of active nonmuscle

myosin filaments (Section 1.2.3). In wild-type embryos, LET-502 is highly expressed in the seam cells, where its high activity could promote myosin-mediated contraction of F-actin (Figure 5). In *let-502* hypomorphic mutant embryos (partial loss of gene function), the seam cells remain cuboidal in shape and fail to elongate, presumably due to the lack of myosin contraction (Piekny et al., 2000). Rho kinase is a RhoA effector in other eukaryotes, however, due to the lack of *rho-1* mutants, *rho-1* had not been shown to be involved in the elongation pathway. Showing that *rho-1* is also required in the seam cells for elongation would support the hypothesis that LET-502's (a Rho effector) activity is high in these cells to promote nonmuscle myosin phosphorylation.

Conversely, myosin phosphatase likely promotes myosin relaxation through the dephosphorylation of MLC-4, via the regulatory subunit, MEL-11 (Section 1.2.3). MEL-11 is highly expressed in the dorsal and ventral epidermal cells, and could ensure that myosin activity remains low in these cells (Figure 5; Wissmann et al., 1997; Wissmann et al., 1999). Furthermore, the localization of MEL-11 changes in seam cells, where it becomes sequestered to the boundaries of cells and away from the actin-myosin filaments (Piekny et al., 2003). Hypomorphic *mel-11* mutant embryos have excess tension, likely due to the high levels of myosin contractility in all epidermal cells, which causes embryos to rupture during elongation (Wissmann et al., 1999; Piekny et al., 2000). Furthermore, RGA-2 is a RhoGAP that promotes the hydrolysis of RHO-1-GTP to RHO-1-GDP and is highly expressed in the dorsal and ventral cells (Diogon et al., 2007). *rga-2* mutant embryos display rupture phenotypes similar to *mel-11*, likely caused by hypercontractility of the epidermal cells, supporting that RHO-1 is differentially regulated in the seam cells to promote elongation (Diogon et al., 2007).

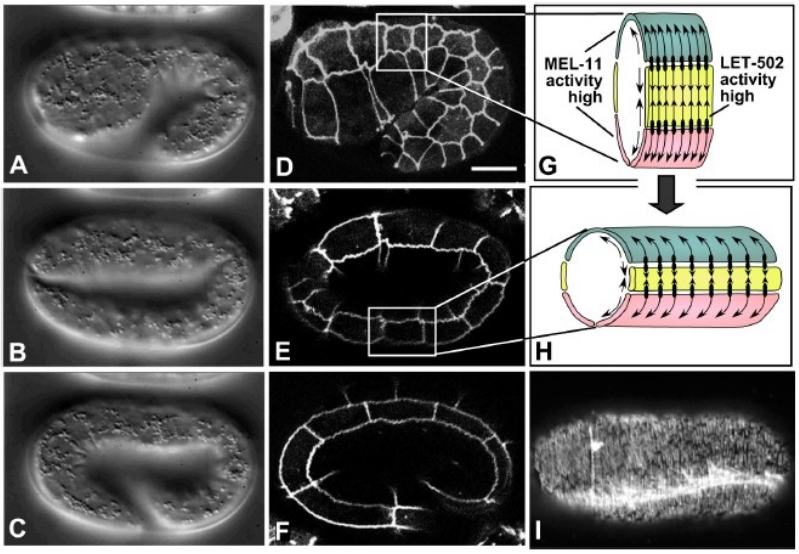

Figure 5. Elongation in *C. elegans*. Nomarski images (left; A-C), DLG-1::GFP images (middle; D-F), cartoon schematics (top right; G,H) and phalloidin-staining (bottom right; I) of a wild-type embryo undergoing elongation of the epidermis. The lateral epidermal cells (seam cells; yellow) have high levels of LET-502 (Rho kinase) and presumably high activity while the dorsal (green) and ventral epidermal cells (pink) have high levels of MEL-11 (myosin phosphatase regulatory subunit) and presumably high phosphatase activity. This would lead to myosin contraction in the seam cells, and relaxation in the dorsal and ventral cells, permitting the seam cells to change from cuboidal in shape to cylindrical as visualized by the DLG-1::GFP localization. Figure from Chisholm and Hardin, (2005).

In support of their antagonistic functions, *let-502* and *mel-11* mutants suppress one another, and double mutant embryos elongate near normally (Wissmann et al., 1997; Piekny et al., 2000). This interaction suggests that the balance of myosin activity is crucial for proper elongation, while other pathways appear to regulate myosin activity in the absence of both *let-502* and *mel-11*.

1.2 Molecular regulators of the cytoskeleton

1.2.1 Rho GTPases

The cytoskeleton is comprised of various filament systems including microfilaments (actin) and microtubules, and is present in all eukaryotic cells to provide them with shape and structure. The main regulators of actin cytoskeletal dynamics are Rho GTPases, including RhoA, Rac and Cdc42. They are often referred to as "molecular switches" as they undergo changes in conformation when they are in their active, GTP-bound state and bind to effectors to drive many cellular processes such as cell division, morphogenesis and cell migration (Hall et al., 1998). Guanine nucleotide exchange factors (GEFs) activate GTPases by promoting the exchange of GDP for GTP (Reviewed by Rossman et al., 2005). GTPase activating proteins (GAPs) hydrolyze GTP to GDP and inactivate GTPases (Reviewed by Tapon and Hall, 1997). RhoA regulates formation of stress fibres and the contractile ring for cytokinesis (Figure 6), which occurs at the end of mitosis to separate a cell into two daughter cells. Active RhoA directs the formation of long, unbranched actin filaments that are bundled for stress fibres and are incorporated into the actin-myosin contractile ring (Figure 6; Hall, 1998; Piekny et al., 2005). Rac regulates cortical ruffling and cell migration by mediating the formation of short,

branched actin filaments (Ridley et al., 1992). These filaments form at the leading edge of migrating cells and form lamellipodia that move cells over a substrate (Ridley et al 1992; Reviewed by Hall, 1998). Cdc42 regulates the formation of filipodia, which are also actin-rich protrusions that extend out from cells to help them probe their environments (Mackay et al., 1995).

Active RhoA regulates actin-myosin contraction for cytokinesis and cell shape changes in morphogenesis. In dividing mammalian cells, microtubules dictate the position of the equatorial plane, which is the site of contractile ring formation, ingression and abscission (Reviewed by Glotzer, 2001; Piekny et al., 2005). RhoA is activated by the GEF, Ect2, which is recruited to the central spindle by binding to the GTPase Cyk-4, part of the centralspindlin complex that regulates central spindle formation (Figure 6; Reviewed by Piekny et al., 2005). The recruitment of Ect2 to the central plane of the cell leads to the activation of RhoA in the overlying equatorial cortex to trigger contractile ring formation (Figure 1; Somers and Saint, 2003; Bement et al., 2005; Yuce et al., 2005; a) Zhao and Fang, 2005). Active RhoA binds to downstream effectors, including formins and profilins that nucleate long, unbranched F-actin (Reviewed by Kovar, 2006) and Rho kinase that activates nonmuscle myosin by phosphorylating its associated light chain on highly conserved Thr18 Ser19 residues (Amano et al., 1996; Yasui et al., 1998; Piekny et al., 2005). These actin-myosin filaments contract to ingress and narrow the cytoplasmic bridge between the two future daughter cells, ultimately separating them. Similarly, cell shape changes for morphogenesis require the formation and contraction of actin-myosin filaments. For example, as described earlier, *C. elegans* elongation occurs due to changes in the lateral epidermal cells, which change shape from cuboidal to cylindrical (Section

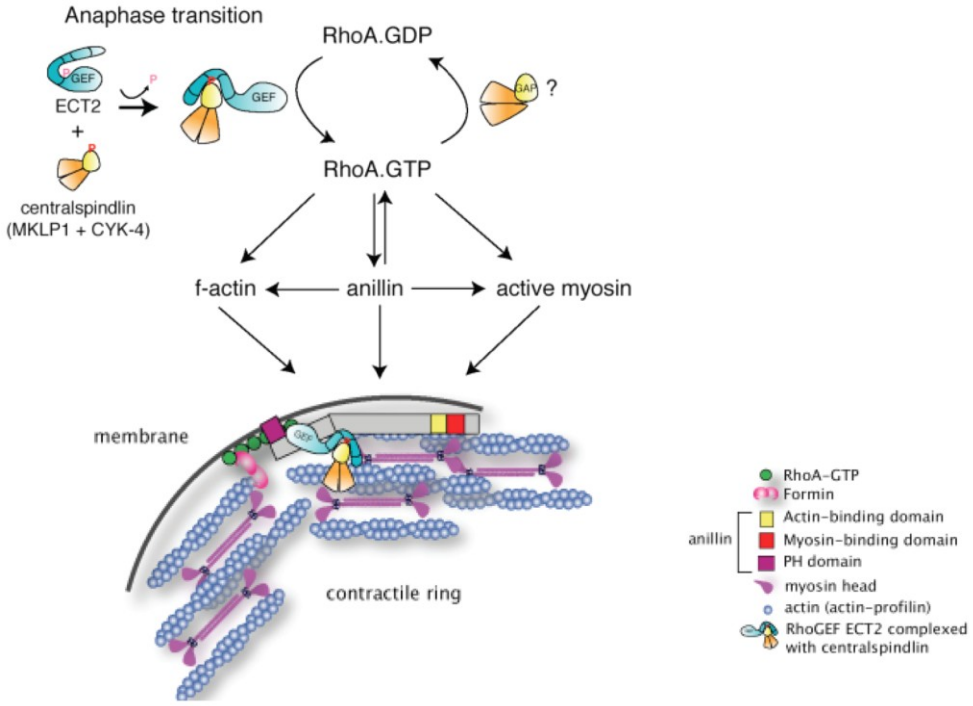

Figure 6. The pathway for cytokinesis in mammalian cells. RhoA activation will regulate its downstream effectors and lead to contractile ring formation and ingression. The onset of anaphase allows for the removal of an inhibitory phosphate on Ect2 (blue), which promotes its binding to Cyk-4, in a complex with Mklp1 at the central spindle (yellow and orange, respectively). Ect2 will activate RhoA (red), which accumulates at the furrow and activates formins (pink) for actin polymerization and activates Rho kinase (ROCK) to phosphorylate regulatory light chain of nonmuscle myosin (rMLC) and activate myosin (purple). Together, actin and active myosin form the contractile ring (light blue). The activation of myosin also promotes ingression of the contractile ring by sliding actin filaments. Figure adapted from Piekny et al., (2005).

1.1.5; Chisholm and Hardin, 2005). LET-502/Rho kinase likely phosphorylates nonmuscle myosin light chain to promote myosin contractility in the seam cells, while MEL-11/myosin phosphatase regulatory subunit removes these regulatory phosphates to inhibit myosin activity in the adjacent dorsal and ventral cells (Figure 7; Wissmann et al., 1997; Piekny et al., 2000; Piekny and Mains, 2002). Recently, the Rho GEF RHGF-2 was shown to be required for elongation of the *C. elegans* embryo, likely to activate RHO-1/RhoA (Figure 7; Lin et al. 2012; Mains, P.E., personal communication). However, despite the requirement for Rho kinase in elongation, a role for RHO-1 has not yet been shown.

The cytoskeleton is also highly regulated to drive cell migrations during morphogenesis. Rac promotes the formation of short, branched actin filaments to form lamellipodia at the leading edge of cells, which helps direct their migration over a substrate (Ridley et al., 1992). Cdc42 promotes the formation of longer actin filaments that form protrusions, also at the leading edge of the cell (Mackay et al., 1995). RhoA also typically contributes to cell migration, but in an antagonistic manner to Rac. It forms long, unbranched actin filaments that are bundled to form stress fibres in the rear of the cell. These fibres associate with nonmuscle myosin to form contractile units. One end of the fiber is adhered to the extracellular substrate by focal adhesions and the force generated by myosin contractility pushes the cell forward (Pestonjamasp et al., 2006). Circumferential bands of actin-myosin also help cells maintain polarity, particularly epidermal cells that form junctions with neighbouring cells near their apical surface (Reviewed by Labouesse, 2006).

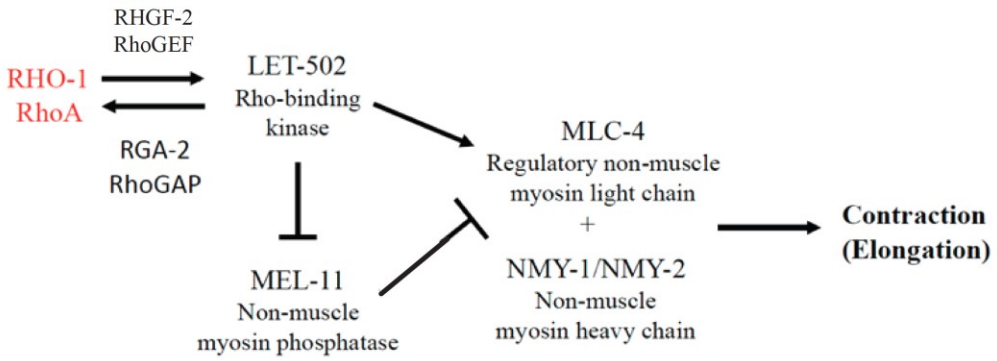

Figure 7. The core pathway for myosin contractility during C. elegans elongation. The predicted upstream regulator of the pathway is RHO-1 (not confirmed). RHO-1 is activated by the GEF RHGF-2 (GEF) and is inactivated by the GAP RGA-2. Active RHO-1 presumably would bind and activate LET-502 (Rho kinase), which phosphorylates MLC-4 (regulatory nonmuscle myosin light chain) to promote the formation and activation of myosin (together with NMY-1/NMY-2 (nonmuscle myosin heavy chain) in the lateral epidermal cells. This drives the contraction of F-actin to change the shape of these cells. LET-502 also phosphorylates and negatively regulates MEL-11 (myosin phosphatase regulatory subunit), an antagonist that removes the regulatory phosphates on myosin. In the dorsal and ventral epidermal cells, high MEL-11 could promote myosin relaxation.

1.2.2 Actin

Actin polymerization is essential for contractile or migration-based events for the morphogenesis of tissues, as well as for cytokinesis. There are two main types of actin filaments; short, branched filaments that direct the ruffling or spreading of membrane during migration and long, unbranched filaments that form contractile units with nonmuscle myosin. Both types of filaments are used by cells during *C. elegans* epidermal morphogenesis (Reviewed by Chisholm and Hardin, 2005). Actin regulators polymerize actin into short, branched filaments by the Arp2/3 complex or long, unbranched filaments through the activity of formins (Pollard et al., 2000; Sawa et al., 2003; Goode et al., 2007; Pollard et al., 2009).

The Arp2/3 complex mimics a core actin complex and acts as a template to nucleate monomeric actin into filamentous actin in a branched manner (Figure 8; Mullins et al., 1998; reviewed by Pollard et al., 2000). The branching of actin filaments occurs when the Arp2/3 complex binds to a pre-existing actin filament and initiates a new daughter strand at a 70° angle (Figure 8; Mullins et al., 1998). The complex is comprised of seven subunits and Arp2 binds to the mother filament, while Arp3 recruits monomeric actin to create a new filament (Welch et al., 1997). WASp (Wiskott-Aldrich Syndrome protein) and Wave/Scar (WASp family Verprolin-homologous in vertebrates/ Suppressor of cAMP Receptor in Drosophila) complexes bind to the Arp2/3 complex to promote actin nucleation (Figure 8; Symons et al., 1996; Machesky and Insall, 1998). WASp is held inactive by auto-inhibition between two domains in its C-terminus, one of which is a Rho GTP-binding domain (GBD). Cdc42-GTP activates WASp by binding to its GBD,

relieving inhibition of the second domain in the C-terminus and rendering it available for Arp2/3 binding (Torres et al., 2006). The Wave protein (GEX-1 in *C. elegans*; Soto et al., 2002) in the Wave/Scar complex shares homology with WASp in its C-terminus but lacks the GBD and is regulated in a different manner (Kurisu et al., 2009). Wave/Scar is a pentameric complex comprised of Abi (Abl interactor protein), Kette/Nck-associated protein 1 (Nap1), Sra1 (Specifically Rac1-associated protein) and Brk1/Hspc300 (Breast tumor kinase/hematopoietic stem/progenitor cell protein 300) that can be activated by Rac. Sra1 and Kette/Nck-associated protein 1 have homologues in *C.elegans;* GEX-2 and GEX-3, respectively (Patel et al., 2008). During myoblast fusion, active Rac binds to the Abi/Nap1 complex, which changes their affinity for the C-terminus of Wave, releasing a binding domain for the Arp2/3 complex and promoting F- actin polymerization for cortical ruffling (Kurisu et al., 2009; Abmayr and Pavlath, 2012).

Formins are RhoA effector proteins that regulate actin polymerization, together with profilins, by nucleating G-actin into F-actin. Formins (CYK-1 in *C. elegans*; Swan et al., 1998) consist of a proline-rich Formin Homology 1 domain (FH1), which binds profilins and a highly conserved Formin Homology 2 domain (FH2), which homodimerizes and is required for actin polymerization by associating with the barbed growing end of the actin filament (Evangelista et al., 2002; Paul et al., 2009). Formins are autoinhibited by association of the N-terminal Diaphanous Autoregulatory Domain (DAD) with the C-terminal DAD-interacting domain (DID). A GBD (Rho-GTP binding domain) overlaps with the DID and Rho-GTP binding relieves the autoinhibition (Alberts, 2001; Kovar, 2006). In other words, formins can be activated through RhoA-GTP binding to the GBD, which will expose the core FH1 and FH2 domains for actin

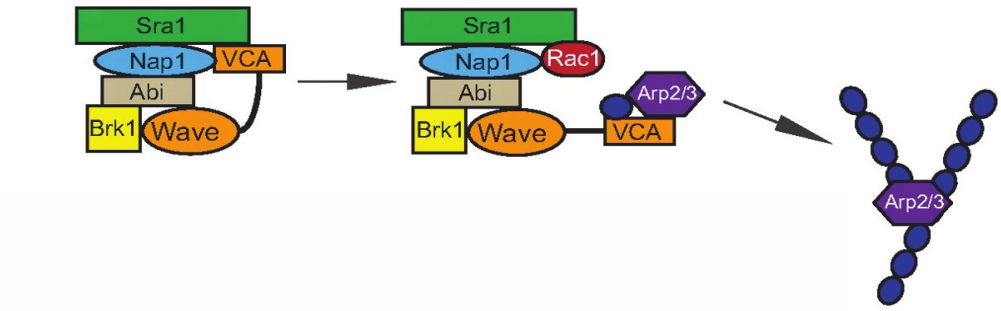

Figure 8. Arp2/3 nucleation of F-actin. The Arp2/3 complex promotes the formation of branched actin filaments. Arp2/3 will be activated by nucleation-promoting factors such as the Wave/Scar complex, comprised of five proteins. The C-terminus of Wave (orange), which contains the Arp2/3 binding site, is bound to Nap1 (blue) and Sra1 (green), keeping it inactive. Active Rac1 (red) competes for this binding on the Nap1/Sra1 complex, freeing the C-terminal (VCA) portion of Wave so it can bind to Arp2/3. This helps promotes Arp2/3-mediated nucleation of branched F-actin, by binding to a pre-existing actin filament and nucleating novel actin filaments at an angle. Figure adapted from Abmayr et al., (2012).

polymerization (Li et al. 2005; Kovar, 2006). Two FH2 domains bind together to form a donut like structure that encircles the growing end of the actin filament, while the FH1 domains extend from the donut to recruit profilin-G-actin complexes and increase the rate of polymerization (Kovar, 2006; Reviewed by Pollard et al. 2009).

1.2.3 Myosin

The formation and activation of non-muscle myosin filaments is essential for ingression of the contractile ring during cytokinesis and for cell shape changes during morphogenesis. Nonmuscle myosin II is an actin-binding protein capable of generating force by sliding actin filaments (Reviewed by Vicente-Manzanares et al., 2009). Nonmuscle myosin II contains a pair of heavy chains, each with an N-terminal motor domain and a long coiled coil region that multimerizes, and two pairs of light chains, the regulatory (RLC) and essential chains, that associate with the neck region of the heavy chain (Somlyo and Somlyo, 2000; Vincente-Manzanares et al., 2009). The regulatory light chains are phosphorylated on highly conserved Thr18 Ser19 residues, which is required for the formation of active myosin filaments and to regulate it's activity (Craig et al., 1983; Vincente-Manzanares et al., 2009). Several kinases have been shown to phosphorylate RLCs in vitro including myosin light chain kinase (MLCK; Somlyo and Somlyo, 2000), Rho kinase (Amano et al., 1996; Totsukawa et al., 2000) and Citron kinase (Yamashiro et al., 2003), although it is not clear how they function in vivo. Myosin phosphatase downregulates myosin activity by removing phosphates on Thr and Ser, and opposes the activity of myosin kinases. Rho kinase also has been shown to phosphorylate the regulatory subunit of myosin phosphatase, rendering the phosphatase

inactive (Kimura et al., 1996; Kawano et al., 1999; Somlyo and Somlyo, 2000). In *C. elegans*, loss of Rho kinase causes embryonic phenotypes consistent with hypocontractility and mutations in the myosin phosphatase regulatory subunit cause phenotypes consistent with hypercontractility. Double mutants carrying mutations in each of these genes suppress these phenotypes, supporting that they function antagonistically in vivo (Figure 2; Wissmann et al., 1997; Piekny et al., 2000).

1.2.4 Anillin

The actin-myosin cytoskeleton is highly regulated to control contractile events for cell shape changes. Anillin is a highly conserved scaffolding protein that organizes actin-myosin contractility and is best known for its function in cytokinesis (Figure 9; Field et al., 1995; Straight et al., 2005; Goldbach et al., 2010; Reviewed by Piekny and Maddox, 2010). During cytokinesis, the contractile ring is made of long, unbranched actin filaments that slide by nonmuscle myosin motor activity to close the contractile ring via a purse-string mechanism (Matsumura, 2005; Piekny et al., 2005). Active RhoA is generated at the equatorial plane and recruits anillin (Oegema et al., 2000; Hickson et al., 2008; Piekny et al., 2008). In addition to its N-terminal myosin and actin binding domains, anillin has a C-terminal anillin homology domain (AHD) that binds to RhoA and Ect2 (human cells; Frenette et al., 2012) or RacGAP50C (Drosophila Cyk-4 homologue; D'Avino et al., 2008; Gregory et al., 2008) and a pleckstrin homology domain (PH) that binds to septins (Oegema et al., 2000; Field et al., 2005; Maddox et al., 2007). Through these structural features anillin crosslinks the actin-myosin cytoskeleton to key components of the division plane including the mitotic spindle (via Ect2 or

RacGAP50C) and the membrane (directly or via septins; Piekny and Maddox, 2010). Several studies have shown that anillin is essential for cytokinesis in human and *Drosophila* cells. In these cells, contractile rings form and ingress, but become laterally unstable after its depletion and oscillate prior to regressing (Straight et al., 2005; b) Zhao and Fang, 2005; Piekny et al., 2008; Hickson et al., 2008; Goldbach et al., 2010).

The genome of *C. elegans* encodes three different genes for anillin: *ani-1*, *ani-2* and *ani-3* (Figure 9; Maddox et al., 2005) The ANI-1 isoform shares conservation with other metazoan anillin's throughout its length, while ANI-2 and ANI-3 share conservation only in their C-termini (Figure 9; Maddox et al., 2005). Thus, while all three anillin isoforms have the AHD and PH domain, only ANI-1 can also bind to actin and myosin, and is the focus of my studies. *ani-1* is required for actin-myosin organization and contractility in the early embryo and promotes asymmetric furrow ingression (Maddox et al., 2005; Maddox et al., 2007). Unlike mammalian cells, cytokinesis often does not fail in *ani-1*-depleted *C. elegans* embryos. However, these embryos are sensitized for cytokinesis defects when other components of the contractile ring are perturbed (Maddox et al., 2007). Additionally, embryos with reduced levels of *ani-1* fail to extrude their polar bodies leading to meiotic defects (Maddox et al., 2007; Dorn et al., 2010). Adults derived from *ani-1*-depleted embryos exhibit body morphology phenotypes consistent with roles for *ani-1* in the morphogenesis of tissues (Maddox et al., 2005). However, previous studies did not investigate roles for *ani-1* during mid-late embryogenesis.

1.2.5 Adhesion complexes

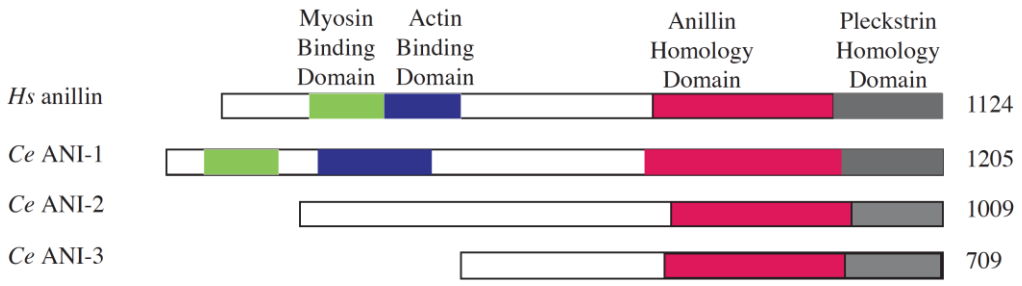

Figure 9. Anillin homologues and isoforms. Alignments of anillin isoforms from Human, *Drosophila* and *C.elegans*. Shown are the conserved Myosin Binding Domain (green), Actin Binding Domain (blue), Anillin Homology Region (pink), which binds to RhoA and Ect2 (human) or RacGAP50C (Drosophila), and the Pleckstrin Homology Domain (grey), which binds to septins. Note that of the *C. elegans* isoforms, only ANI-1 contains myosin and actin binding domains in addition to the C-terminal domains. Figure adapted from Maddox et al., (2005).

Connections must be made and maintained between the cytoskeleton of neighbouring cells to coordinate cell movements and cell shape changes during the formation of a tissue. These connections are composed of adhesion complexes, which crosslink the internal actin cytoskeleton to neighboring cells and helps define their polarity. Epithelial adhesion complexes contain E-cadherin, a calcium-dependent cell-cell adhesion glycoprotein that interacts with the extracellular domains of other E-cadherins, and α and β catenin that binds to the internal F-actin cytoskeleton (Kobielak et al. 2004; Reviewed by Baum and Georgiou, 2011). In *C. elegans*, epidermal cells are inter-connected by adherens junctions, which are found near the apical surface of cells and are comprised of the catenin-cadherin complex (CCC) and a second, distinct and slightly more basal complex containing DLG-1 and AJM-1 (DAC; Figure 10; Koeppen et al., 2001; Pettitt et al., 2003; Reviewed by Labouesse, 2006). The CCC is made up of HMR-1 (cadherin), HMP-1 (α-catenin), HMP-2 (β-catenin) and JAC-1 (p120 catenin; Figure 5; Costa et al., 1998; Pettitt et al., 2003; Labouesse, 2006). HMR-1 is a transmembrane protein that binds intracellularly to a complex of HMP-2 and HMP-1, which is bound to F-actin and tethers the internal F-actin cytoskeleton to the junction. The extracellular domain of HMR-1 interacts with HMR-1 on an opposing, adjacent cell to form a junction between the two cells (Figure 10; Costa et al., 1998; Pettitt et al., 2003). During *C. elegans* ventral enclosure (Section 1.1.4), migrating ventral epidermal cells extend actin rich filopodia and migrate to meet their contralateral neighbours at the ventral midline where they form novel adherens junctions (Raich et al., 1999). The junctions also help promote the

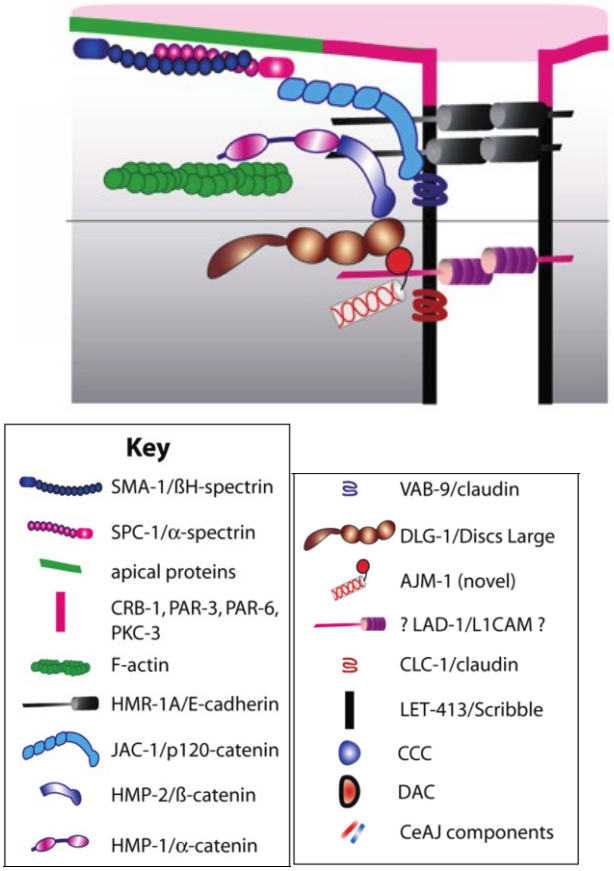

Figure 10. A schematic of an adherens junction in a *C.elegans* epidermal cell. The more apical portion is the CCC (cadherin/catenin complex). The internal F-actin cytoskeleton (green) binds to HMP-1 (α-catenin; pink). HMP-1 and HMP-2 (β-catenin; purple) form a complex that binds to HMR-1 (E-cadherin; black). The extracellular portion of HMR-1 forms a dimer with HMR-1 proteins on a neighbouring cell to connect adjacent cells to each other. Also shown is the more basal DAC (DLG-1/AJM-1 complex). Adapted from Labouesse, (2006).

extension of more filopodia to continue to drive cell movements. Zygotic *hmr-1* mutants and maternal/zygotic *hmp-1* or *hmp-2* mutants show similar phenotypes, where the migration of ventral epidermal cells initiates normally, but cells fail to form junctions as they meet near the ventral midline. The internal contents of these embryos extrude (via rupture of the epidermal tissue) or embryos hatch and have abnormal body morphologies (Costa et al., 1998; Raich et al., 1999; Reviewed by Chisholm and Hardin, 2005). Mutations in the DAC components do not cause strong phenotypes, but display bubbling between neighboring epidermal cells, suggesting a defect in cell adhesion (Koeppen et al., 2001; Labouesse, 2006), however, they likely are partially redundant with the CCC.

1.3. Summary

The formation of tissues in vivo is highly complex and involves a myriad of events that are still poorly understood. This thesis describes the role of *rho-1* and *ani-1* in epidermal morphogenetic events during *C. elegans* embryogenesis. Although the role of nonmuscle myosin regulators, such as Rho kinase/LET-502, had been described for elongation, RhoA had not been studied due to the lack of alleles. Using a deletion allele of *rho-1* generated by the *C. elegans* Knockout Consortium, genetic crosses and live imaging were performed to show the zygotic function of *rho-1.* As predicted, *rho-1* functions in the same pathway as *let-502* and *mlc-4*, likely as an upstream regulator to drive myosin contractility for elongation of the embryo.

The remainder of this thesis revealed a novel role for *ani-1* in ventral enclosure. First, *ani-1* is required throughout embryogenesis and RNAi gives a range of morphogenetic phenotypes, including ruptured embryos and misshapen larvae. Further

phenotypic analyses revealed that *ani-1* is required for the migration and/or adhesion of ventral epidermal cells during ventral enclosure. The expression of ANI-1 in the underlying neuroblasts suggests that *ani-1* functions non-autonomously. It is not clear how the neuroblasts regulate migration of the overlying ventral epidermal cells, and this data suggests that at least one mechanism may be mechanical. The effects of changing myosin contractility (and tension) on ventral enclosure, by combining mutant components of the *rho-1* pathway with *ani-1* RNAi, revealed that altering epidermal tension influences the efficiency of ventral enclosure.

Chapter 2. Materials and Methods

2.1. Strains and Alleles

C. *elegans* strains (var. Bristol) were maintained according to standard protocol (Brenner, 1974) on NGM (nematode growth media – for 1L; 3g NaCl, 17g Agar, 2.5g BactoPeptone, 1mL 1M $CaCl_2$, 1mL 1M $MgSO_4$, 1mL of 5mg/mL cholesterol solution and 25 mL of 1 M PPB or KPO_4 buffer). NGM plates were each seeded with ~100µl *Escherichia coli* (*E. coli*) OP50.

The following strains were obtained from the *Caenorhabditis* Genetics Center (CGC): N2 (wild type), *rho-1 (ok2418)/nT1[qIs51], dpy-4 (e1166), mlc-4 (or253)/qC1, nmy-1 (sb115), mel-11 (it26) unc-4 (e120) sqt-1 (sc13)/mnC1, ajm-1 (ok160); jcEx44[ajm-1::GFP + pRF4 (rol-6 (su1006)] and unc-119 (ed3); tjIs1 [pie-1::GFP::rho-1 + unc-119 (+)]*. The following strains were obtained from P.E. Mains (University of Calgary)*: rhgf-2 (sb100) and let-502 (sb118).* GFP::ANI-1 and GFP::HMR-1 were obtained from A. S. Maddox (IRIC, University of Montreal). S. Jenna (UQUAM, Montreal) kindly provided us with the following strains; *rde-1 (ne219)/kzls8, rde-1 (ne219)/kzls9* and *rde-1 (ne219)/kzls20* (the same strains also were ordered from the CGC). The *vab-2* (*quEx16)* and *vab-1 (vab-1 (e2); juls53*) lines were obtained from I. Chin-Sang (Queen's University, Kingston). The following strains were made for this study: *rho-1 (ok2418)/dpy-4 (e1166) and rho-1 (ok2418)/+; jcEx44. C. elegans* strains were maintained on NGM (Brenner 1974). All temperature sensitive strains were maintained at 15°*C*.

2.2. Genetic Crosses

C. elegans are hermaphrodites (x/x) or males (x/o), making this organism a suitable model for carrying out genetic crosses. Broods were scored as described by Mains et al., (1990) to assess genetic interactions, which is described briefly here. Eight to ten male worms and two L4-staged hermaphrodites were placed on an NGM plate and left overnight for mating. After approximately 24 hours, or when the brood size was about 30 eggs, mothers were each transferred to separate NGM plates (males were either transferred with the mothers or discarded), and transferred every 24 hours to a fresh plate. In order to confirm that mating had occurred properly, offspring were screened for the frequency of males (typically <0.1%, but after outcrossing is ~50%). Unless sterility was an issue, hermaphrodites had total brood sizes of 2-300 progeny. Temperature sensitive strains such as *mel-11*, *let-502* or *rhgf-2* were maintained at 15°C and upshifted to 20°C or 25°C at the L4 stage for experimental observations. Phenotypes were assessed as indicated in the tables. Genetic interactions were determined using the Chi-square test, based on predicted frequencies of genotypes and phenotypes for independently segregating alleles.

2.3. RNAi

RNA-mediated interference was used to knockdown the levels of specific gene products and was performed using feeding vectors obtained from the RNAi library described in Fraser et al., (2000) and Kamath et al., (2003). For this study, clones specific for *rho-1* (Y51H4A.3) and *ani-1* (Y49E10.19) were generously provided by M. Glotzer

(University of Chicago) and A.S. Maddox (IRIC), respectively. RNAi plates were made in the same way as NGM plates (described above) however, IPTG (1mL for 1L) and ampicillin (500uL for 1L) were added. The vector containing the target sequences is called L440, which is Ampicillin-resistant and contains IPTG-inducible RNA polymerase promoters to generate dsRNA (~500bp-1.5kb). Glycerol stocks for the RNAi clones were streaked onto ampicillin LB plates and left to grow overnight. Single colonies were picked and induced overnight (12-16 hours) in 5 mL of LB and 500 uL of ampicillin at 37°C. A subsequent 1:100 dilution (with fresh LB and ampicillin) was made the following day and incubated for 7-9 hours at 37°C. The bacterial solution was then centrifuged at 13000 rpm for 1 minute and the pellet was re-suspended in fresh LB to reduce the volume by 5-fold and obtain a concentrated bacterial solution. Approximately 70 uL of bacterial solution was then plated onto the NGM RNAi plates and left overnight to dry. Worms ingest the bacteria containing the dsRNA, which passes from the gut to the gonads, and during this process siRNAs are generated to degrade the specific target mRNA in the germline.

Eight L4 hermaphrodites were placed onto one RNAi plate for ~24 hours. After, individual worms were transferred to fresh RNAi plates and progeny from these second plates were assessed for phenotypes. The empty L440 vector, which lacks cDNA, served as a negative control (*i.e.,* 0% lethality was expected) while *rho-1* RNAi was used as a positive control (*i.e.,* 100% lethality was expected and eventual sterility should be observed with efficient RNAi). Furthermore, all RNAi experiments were repeated multiple times and the results were recorded separately.

2.4. Immunostaining

2.4.1 ANI-1 Localization

N2 or AJM-1::GFP embryos were fixed and immunostained for ANI-1 and tubulin or GFP. Embryos obtained from gravid adult hermaphrodites dissected in M9 solution were mounted on poly-lysine coated microscope slides, freeze-cracked in liquid nitrogen (coverslips were placed over the area of the slide with the embryos and popped off after freezing) and subsequently fixed in ice-cold methanol (-20 ^{o}C) for 15 minutes. To increase the number of embryos on the slide, gravid adult worms were exposed to bleaching solution (4 mL H_20, 0.4 mL bleach, 0.4 mL 10 M NaOH) and occasionally vortexed before fixing. First, worms were washed off plates with M9 solution (for 10 X concentration; 30 g KH_2PO_4, 60 g Na_2HPO_4 and 50 g NaCl) and transferred with glass pipettes into siliconized 1.5 mL microcentrifuge tubes. The tubes were centrifuged for one minute at 13,000 rpm and the supernatants were discarded. 1 mL of bleach solution (2% bleach, 200 mM NaOH in water) was added to each tube, incubated at room temperature for 3-4 minutes and subsequently centrifuged for another minute. The pellets of embryos were washed three times with M9 solution, then transferred onto poly-lysine coated slides and freeze-cracked in liquid nitrogen. Embryos were fixed with methanol as mentioned above.

After fixing, slides were washed each three times for 10 minutes with 0.1% TBST (150 mM NaCl, 50 mM Tris HCl, pH 7.6 and 0.1% Tween-20). After washing, the slides were incubated with 1:1600 rabbit anti-ANI-1 antibodies (generously provided by A.S. Maddox, IRIC, University of Montreal), 1:250 mouse anti-alpha-tubulin antibodies (DM1A; Sigma) or 1:200 mouse anti-GFP antibodies (Roche), diluted in TBST with 5%

NDS and incubated for two hours at room temperature in a wet chamber. Following this incubation, each slide was washed three times with 0.1% TBST. Subsequently, slides were incubated with secondary antibodies (1:250 anti-rabbit 488 and 1:250 anti-mouse 568 or 488; Invitrogen) for two hours at room temperature. The slides were then washed three times in 0.1% TBST, following an incubation with 1:1000 DNA-binding dye DAPI (1 mg/mL; Sigma) for five minutes at room temperature. After, the slides were each washed once with 0.1% TBST and once with 0.1M Tris HCl pH 8.8. In order to mount the slides, 20 μl of pre-warmed mounting media (5% n-propyl gallate, 50% glycerol, 50 mM Tris, pH 9, 37°C) was applied to each slide. Finally, coverslips were added onto each slide and sealed with colored nail polish.

2.4.2 ANI-1 and VAB-1 or VAB-2 co-staining

Attempts were made to co-stain ANI-1 and VAB-1 or VAB-2 to determine if ANI-1 localizes in neuroblasts. Since both ANI-1 and VAB-1 or VAB-2 antibodies are derived from rabbit, additional steps were taken when performing the staining protocol outlined above. Fixed embryos from gravid hermaphrodites over-expressing VAB-1 or VAB-2 (courtesy of I. Chin-Sang, Queen's University) were incubated with 1:1600 anti-ANI-1 antibodies, then washed three times, and incubated with 1:50 1mg/mL goat anti-rabbit Fab fragment (Affinipure F(ab')2 fragment Goat anti-Rabbit IgG, Jackson ImmnoResearch) for another two hours at room temperature. This changed the identity of the ANI-1 primary antibodies to goat, enabling them to be co-stained with rabbit antibodies to another protein. After washing the slides three times with 0.1% TBST, they were incubated with primary rabbit antibodies to 1:50 VAB-1 or VAB-2 for two hours.

After, washing the slides three times with 0.1% TBST, they were incubated with 1:250 donkey anti-goat 488 and 1:250 donkey anti-rabbit 568 secondary antibodies for one and a half hours and completed as described above.

2.5. Microscopy

2.5.1 Live Imaging

Embryos were collected for live imaging as described in Sulston et al. (1983). The general procedure for collecting embryos and imaging is briefly described. A 2% agarose drop (2% w/v agarose in distilled water) was dispensed onto a pre-warmed microscope slide and another microscope slide was placed perpendicularly on top of the first slide in order to form a flat pad of agarose. After sliding off the top slide, the slide with the pad was used immediately. Approximately ten to fifteen gravid hermaphrodites were placed into the well of a depression microscope slide filled with M9 solution. A scalpel was used to dissect the worms and expel their eggs. The eggs were collected with the use of a glass capillary tube attached to a mouthpiece with rubber tubing for suction and transferred onto the microscope slide with the agarose pad. A coverslip was then placed over the slide and sealed with petroleum jelly to avoid dehydration of the embryos during live imaging.

To assess phenotypes, live embryos were observed by 4D time-lapse microscopy either every 10 minutes, or every 3 minutes depending on the phenotypic analysis. Images were obtained using DIC and/or the GFP excitation-emission filters (for GFP-expressing embryos) with the 40X or 63X objective on a Leica DMI6000B inverted microscope using a Hamamatsu Orca R2 camera and Volocity acquisition software

(PerkinElmer). Z-stacks of 5-10 planes of 1 □m thickness from the surface to medial planes of the embryo were collected using the Piezo Z/ASI stage (MadCityLabs). Phototoxicity, caused by the exposure of embryos to UV light, was prevented by closing the aperture to 30%. Moreover, exposure times were kept below 150 ms (compensated by increasing gain up to 150). ANI-1::GFP embryos were imaged using the 60X objective on an inverted Nikon Eclipse Ti microscope outfitted with the Livescan Sweptfield scanner (Nikon), Piezo Z stage (Prior) and the Andor Ixon 897 camera, using Elements 4.0 acquisition software (Nikon). Some phenotypes were initially determined by imaging embryos by Nomarski using the 40X or 60X objectives on an upright Nikon Optiphot-2 microscope using a Nikon Digital DS-Fi1 camera.

2.5.2 Imaging Fixed Samples

Images from fixed embryos were collected using excitation/emission filters for GFP, Texas Red and DAPI and the 63X objective on a Leica DMI6000B inverted microscope with a Hamamatsu Orca R2 camera and Volocity acquisition software (PerkinElmer). Z-stacks of 0.2-0.5 □m thickness were collected through the entire embryo using the Piezo Z/ASI stage (MadCityLabs). Images were also collected using the 63X objective on a Leica TCS SP2 confocal microscope with spectral detector and Leica confocal software V1.4.

2.5.3 Images for Figures

Images were exported from either Volocity or Elements into TIFFs and then opened in Image J (NIH). Selected Z planes and time points were chosen, cropped,

rotated and converted into 8-bit images, which were then imported into Adobe Photoshop and Illustrator to compile figures. Maximum intensity Z-stack projections were made using selected planes. Quicktime (Apple) movies were generated in Image J using selected time points of Z-stack projections after cropping and rotating the original images.